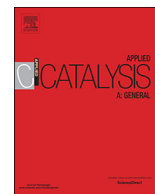




ELSEVIER

Contents lists available at ScienceDirect

Applied Catalysis A, General

journal homepage: www.elsevier.com/locate/apcata

Selective conversion of biomass-derived levulinic acid to ethyl levulinate catalyzed by metal organic framework (MOF)-supported polyoxometalates

Tianmeng Guo, Mo Qiu, Xinhua Qi*

Agro-Environmental Protection Institute, Chinese Academy of Agricultural Sciences, No. 31, Fukang Road, Nankai District, Tianjin, 300191, China

ARTICLE INFO

Keywords:

Levulinic acid
Biofuel
Esterification
Metal-organic frameworks
Polyoxometalates
Biomass

ABSTRACT

The esterification of levulinic acid (LA) and ethanol into ethyl levulinate is an attractive biomass conversion process since the product EL has wide applications as food additive, fragrance and fuel. Herein, a metal-organic framework (MOF)-supported phosphomolybdic acid [Cu-BTC][HPM] was synthesized with 1,3,5-Benzenetricarboxylic acid, copper nitrate and phosphomolybdic acid in a one-step process at ambient temperature. The synthesized [Cu-BTC][HPM] was used for the catalytic esterification of levulinic acid to EL in ethanol, and showed excellent activity with a high EL yield close to 100% at 120 °C for 6 h, which should be ascribed to the uniform dispersion of HPM embedded in the MOF. The [Cu-BTC][HPM] catalyst could keep stable crystal structure and active component contents, and thus exhibited good stability in recycling process.

1. Introduction

With the gradual depletion of fossil fuels and the increasing demand for energy, it is urgent to develop renewable and sustainable energy resources to meet current need for fine chemicals, chemical materials and fuels [1–5], among which, biomass, as one of the renewable resources with abundant reserves and widespread distribution, has attracted significant attention. Levulinic acid (LA), a high value-added chemical derived from biomass, can be obtained from cellulose by acid-catalyzed hydrolysis process [6]. Since it's an organic acid with both ketone carbonyl and carboxyl groups, it has good reaction activity and can be used to produce levulinate esters, γ -valerolactone, 2-methyltetrahydrofuran and other fuel additives through various reactions such as esterification, redox, substitution and polymerization [7–9]. Among various products, ethyl levulinate (EL) is particularly worthy of attention, since its physicochemical properties are similar to fatty acid methyl esters in biodiesel, and it can be used as a new liquid fuel additive to partially replace petroleum. In addition, it's also an important chemical feedstock for the production of food flavor [8,10,11].

EL can be efficiently produced by esterification of LA with ethanol [12] (Scheme 1). In previous studies, inorganic acids such as sulfuric acid [13], hydrochloric acid, and p-toluenesulfonic acid have been widely used in esterification reactions to achieve high yields. However, these conventional homogeneous catalysts inevitably have disadvantages such as difficulty in recycling, equipment corrosion, and environmental pollution [10]. In contrast, heterogeneous catalysts are

generally environmentally friendly and are easily separated from reaction system, which can be a substitute for homogeneous catalysts.

Common solid acids used for esterification include sulfonated zirconium dioxide [14], zeolites [15], heteropoly acids (HPAs) [16], etc. Kuwahara et al. [14] designed a series of sulfated zirconia catalysts with different amounts of silicon. When a 10 wt.%-Si catalyst was used, the conversion of LA reached 77.5% at 70 °C in 10 h reaction time. The study also showed that the catalysts with extremely high acid amounts/densities wasn't the most effective catalyst for the reaction, leading to a conclusion that in addition to the amount of acidic sites, the availability of acid sites determined by the structural properties of the catalytic materials, and the accessibility between the reaction substrate and the acid site were also key factors affecting the catalytic effect. Among them, heteropolyacids are highly valued due to their high proton mobility, stability, fast electron transfer capability and excellent physicochemical structure. Especially for Keggin type HPAs, usually show stronger Bronsted acidity compared with traditional mineral acids [17–19]. Nevertheless, relatively small surface areas and the high solubility of HPAs in polar solvents limit their applications in liquid-phase reactions to a certain extent. Considering the above drawbacks, it is of great significance to search structurally stable carriers to stabilize the HPAs. In this way, the catalyst can be conveniently separated from the reactants and the recyclability is enhanced. Nandiwale et al. synthesized a catalyst loading 15% (w/w) DTPA (dodecatungstophosphoric acid, one kind of HPAs) on H-ZSM-5 (zeolite), which showed good performance in the esterification process of LA with 94% LA conversion

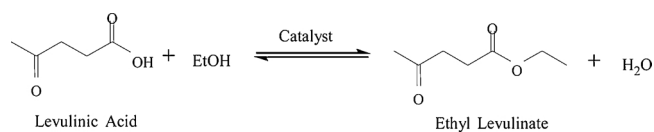
* Corresponding author.

E-mail address: qixinhua@nankai.edu.cn (X. Qi).<https://doi.org/10.1016/j.apcata.2019.01.004>

Received 23 September 2018; Received in revised form 7 January 2019; Accepted 9 January 2019

Available online 09 January 2019

0926-860X/ © 2019 Published by Elsevier B.V.



Scheme 1. Esterification of LA with ethanol into EL.

and 100% EL selectivity [20]. A series of zirconia-supported catalysts with different mass ratios of phosphotungstic acid were tested for EL production. The results showed that under optimal conditions, 97.3% of EL yield can be observed [21].

In recent years, as a new type of multifunctional porous material, metal organic framework (MOF) has attracted much attention due to its novel structure, good stability, and uniformity of pore structure. It has a wide range of applications in gas adsorption, storage and separation, especially in the field of catalysis [22–24]. Ligand-functionalized MOFs have been used to esterification [25]. Given the good pore structure characteristics of MOF, it should be an excellent support for the active ingredient for the esterification reaction. Therefore, in this work, Cu-BTC (Cu^{2+} as the coordination metal, benzene-1,3,5-tricarboxylate as the ligand) loaded with phosphomolybdic acid (HPM) was used for the esterification of LA. Cu-BTC (HKUST-1) was first synthesized with 1,3,5-Benzenetricarboxylic acid and copper nitrate in a mixture of ethylene glycol and water by Chui et al. [26]. Since then many scientists have conducted in-depth research on it. Compared to the other MOFs materials, Cu-BTC has suitable pore size for HPM. Thus, the active ingredient HPM can be immobilized within the pores of the MOF, which should contribute greatly to the stability and recyclability of the catalyst.

2. Experimental

2.1. Chemicals and reagents

Copper acetate monohydrate (99.95%), L-glutamic acid (99%), levulinic acid (99%) were obtained from Shanghai Macklin Biochemical Co., Ltd. (Shanghai, China). 1,3,5-Benzenetricarboxylic acid (99%) was bought from Beijing Innochem Technology Co., Ltd. (Beijing, China). Phosphomolybdic acid hydrate (AR) was received from Shanghai Yuanye Biological Technology Co., Ltd. (Shanghai, China). Ethyl alcohol (99.8%) was provided by Concord Technology Co., Ltd. (Tianjin, China). All chemicals were directly used without further purification.

2.2. Preparation of Cu-BTC and [Cu-BTC][HPM]

In a typical preparation process, 1 mmol copper acetate monohydrate, 0.5 mmol L-glutamic acid and 300 mg of phosphomolybdic acid hydrate were added to 40 ml of distilled water, and the mixture was stirred vigorously to get a clear solution. Then, 140 mg of 1,3,5-benzenetricarboxylic acid dissolved in 40 ml of ethanol was added to the previous prepared solution while stirring continuously. After that, the mixed solution was stirred for 12 h with magnetic stirring to obtain a blue-green precipitate, named as [Cu-BTC][HPM]. For comparison, Cu-BTC was also obtained by the same method, but no phosphomolybdic acid was added during the preparation. After these two precipitates were separated from the solution by centrifugation, the samples were washed with ethanol for three times and dried in a vacuum oven at 70 °C overnight.

2.3. Characterization of the catalysts

The crystallographic information was obtained by the powder X-ray diffraction (XRD) with a Japan Rigaku D/MAX-2500 X-ray diffractometer (Cu $\text{K}\alpha$ radiation, 40 kV, 100 mA). Elemental composition of the catalysts was determined by ICP-OES on an Agilent 730 ICP-OES

instrument. The Fourier-transformed infrared spectroscopy (FTIR) spectrum of the catalyst was observed using a Nicolet iN10 micro-infrared spectrometer. The scanning electron microscope (SEM) images were obtained on a Gemini Sigma 300 scanning electron microscope. The transmission electron microscope (TEM) images and the distribution of elements were characterized using a JEOL JEM-2010 transmission electron microscope with energy-dispersive X-ray spectroscopy (EDX). N_2 adsorption-desorption isotherms were measured at 77 K using a Micromeritics ASAP 2020, and the specific surface area and pore size distribution of Cu-BTC and [Cu-BTC][HPM] were analyzed by the Autosorb IQ analyzer from Quantachrome Instruments, using the Brunauer-Emmett-Teller (BET) method, the Barrett-Joiner-Halenda (BJH) formula (for [Cu-BTC][HPM]) and the Horvath-Kawazoe (HK) formula (for Cu-BTC).

2.4. The procedure for the catalytic esterification of LA to EL

In a typical experiment, a certain amount of LA (0.25 mmol, 0.5 mmol, 1 mmol and 2 mmol) was dissolved into 10 ml ethanol, then the mixture was transferred to a 50 ml Teflon lined stainless steel autoclave followed by the addition of a certain amount of the prepared catalyst (20 mg, 40 mg and 80 mg). The reaction was carried out with magnetic stirring (1000 r/min) at a given temperature (80 °C, 100 °C and 120 °C) for a period of time (2–14 h). Once the reaction was completed, the autoclave was quickly cooled with ice water to end the reaction. After the solid was separated by centrifugation and diluted with anhydrous ethanol, the supernatant was quantified with a GC (Shimadzu) equipped with an Rtx-1 capillary column (30 m \times 0.25 mm) and a flame ionization detector (FID) with N_2 as carrier gas. The column temperature was 100 °C, and the vaporizer temperature was set to 260 °C.

The yield of ethyl levulinate was calculated by the following formula [27]:

$$\text{Yield of ethyl levulinate} = \frac{\text{molar amount of EL generated}}{\text{initial molar amount of LA added}} \times 100\%$$

The recovered catalyst was washed with ethanol several times for reuse. Each reaction was repeated three times, and the reproducibility of EL yields was within 3% in standard deviation.

3. Results and discussion

3.1. Characterization of the prepared MOF-supported HPM

Normally, the preparation of most of the MOFs is carried out at a high temperature by hydrothermal method. Herein we prepared catalysts Cu-BTC and [Cu-BTC][HPM] which were composed of nanoparticle units by stirring at room temperature according to the literature [28]. When an ethanol solution containing an organic ligand and an aqueous solution containing a metal salt were mixed together, with the rapid deprotonation of ligands, MOF could be instantly generated by self-assembly.

The crystal phases of samples are confirmed by X-ray diffraction (XRD) and showed in Fig. 1. There is nearly no difference of the diffraction patterns between the as-prepared Cu-BTC in this work and that reported in the literature [29], demonstrating that in this way, Cu-BTC could be successfully synthesized under mild room temperature. Comparing the prepared [Cu-BTC][HPM] with the original Cu-BTC, the obvious differences of diffraction peaks appeared in the range of 5–10°. The peaks at around 7° and 9° (2 Theta) had significant decreases in the intensity, corresponding to (200) and (220) crystallographic planes of Cu-BTC, respectively. It was proved that HPM was not simply presented on the surface of the MOF, but also was embedded in the pore cage of the Cu-BTC and affected the crystallization of Cu-BTC, thus led to the changes in the diffraction peak of [Cu-BTC][HPM]. No obvious HPM diffraction peaks indicated that HPM was highly uniformly dispersed

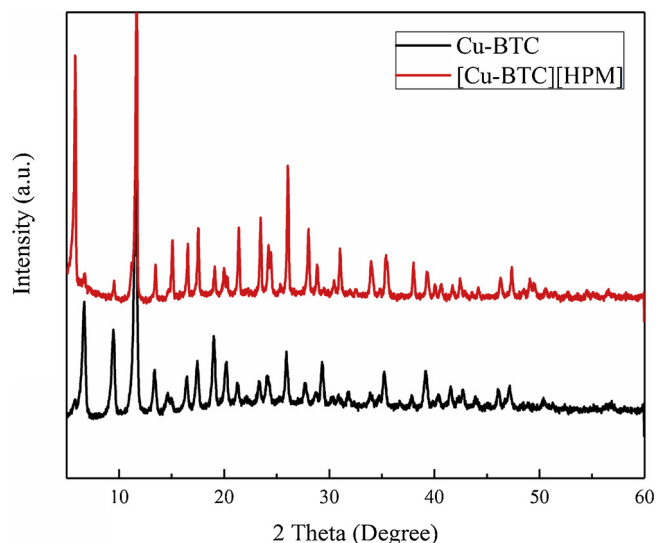


Fig. 1. XRD patterns of Cu-BTC and [Cu-BTC][HPM].

within the MOF structure.

The FT-IR spectra of the Cu-BTC and [Cu-BTC][HPM] samples are illustrated in Fig. 2. The absorption band at 1585 cm^{-1} can be attributed to the stretching vibration of the C=C bond in the benzene ring. The in-plane bending vibration of the C-H in the benzene ring and the C-O-Cu stretching vibration cause absorption bands at 1112 cm^{-1} and 1045 cm^{-1} , respectively [30], while the band around 750 cm^{-1} represents the out-plane bending vibration of the C-H group in the benzene ring. The band at 1644 cm^{-1} can be assigned to the stretching vibration of the C=O in the carboxyl group. The origin of the band at 1448 cm^{-1} is the in-plane bending vibration of the O-H, and the band at 1374 cm^{-1} corresponds to the stretching vibration of the C-O [31,32], which further proves the existence of the carboxyl group. Moreover, the bands at 730 cm^{-1} and 491 cm^{-1} are related to the stretching vibration of Cu-O [33,34], and the absorption bands in the range of $800\text{--}1100\text{ cm}^{-1}$ are the characteristic bonds of HPM [35].

SEM images in Fig. 3 shows the synthesized [Cu-BTC][HPM] consisted of particles roughly 700 nm in average size. As shown in the images, the morphology of these sub-micron-sized particles is typical octahedral structure and truncated octahedral structure. The size and morphology of the synthesized crystals were affected by the acidity and alkalinity of the solution system. Therefore, in the Cu-BTC synthesis

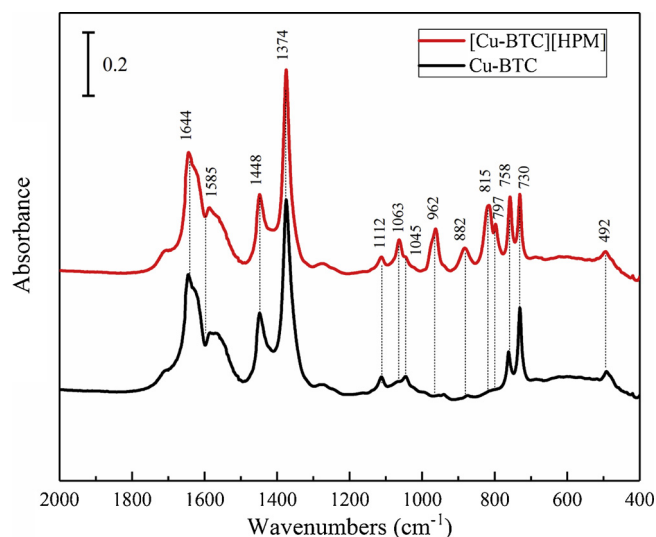


Fig. 2. FTIR spectra of Cu-BTC and [Cu-BTC][HPM].

system without HPM, the crystal nucleation rate was faster, and thus tended to form crystals of smaller particles.

To observe the distribution of Cu, P, and Mo in the catalyst was characterized with EDX mapping (Fig. 4), which further demonstrates that HPM is highly dispersed in the metal-organic framework due to the uniform pore structure of Cu-BTC.

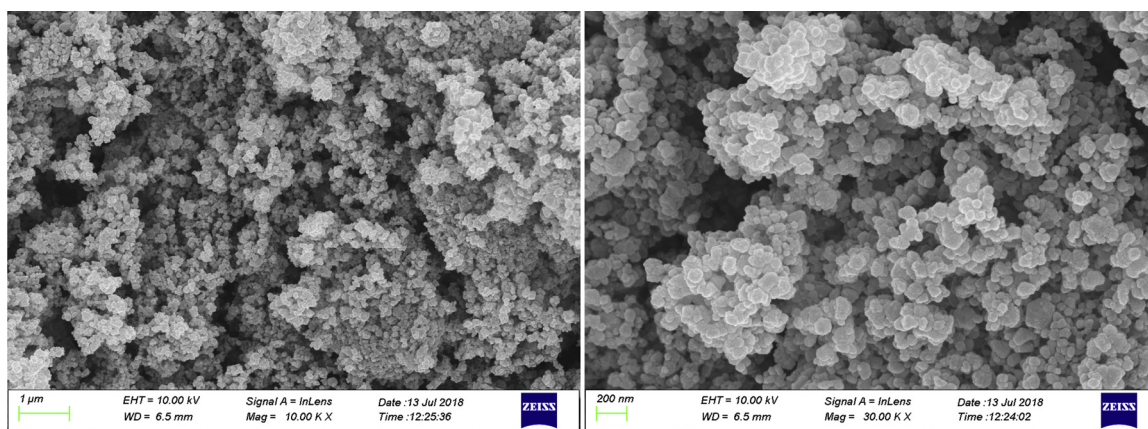
Fig. 5 shows the adsorption-desorption isotherms of Cu-BTC and [Cu-BTC][HPM] samples, which shows that Cu-BTC had the type I isotherm, with specific surface area of $1577\text{ m}^2/\text{g}$. The pore size distribution diagram shows that most of the pore diameters are centred at 0.7 nm within 0–2 nm, which is the ordered microporous structure in Cu-BTC. The hysteresis loop appeared around $p/p_0 = 0.9$ is probably caused by the amorphous pores generated by the interconnection of Cu-BTC particles [36,37], as shown in the meso/macropore size distribution of Cu-BTC in Fig. S1. The nitrogen adsorption-desorption isotherm of the [Cu-BTC][HPM] is a typical type IV isotherm, and there is a significant hysteresis loop at $P/P_0 \sim 0.6\text{--}1.0$, indicating that [Cu-BTC][HPM] had many mesopores. According to the crystal growth theory proposed in References [36,37], the [Cu-BTC][HPM] particles are composed of sub-micron sized particles, and amorphous stacked pores are formed among these particles, corresponding to the existence of amorphous mesopores in [Cu-BTC][HPM]. The addition of HPM influences the synthesis environment, therefore the generated size of ordered pores and amorphous stacked mesopores are also different between [Cu-BTC] and [Cu-BTC][HPM]. Only the ordered pores in Cu-BTC framework can interact with HPM molecules to load them well. Besides, the specific surface of [Cu-BTC][HPM] sharply decreased to $57\text{ m}^2/\text{g}$, which should be ascribed to the introduction of HPM as guests occupied the pores of Cu-BTC, this phenomenon also demonstrates that HPM is embedded in the pores rather than attached to the surface [38]. Table 1 showed the textural properties of Cu-BTC and [Cu-BTC][HPM].

3.2. Effect of reaction time and temperature on the catalytic conversion of LA to EL by [Cu-BTC][HPM] catalyst

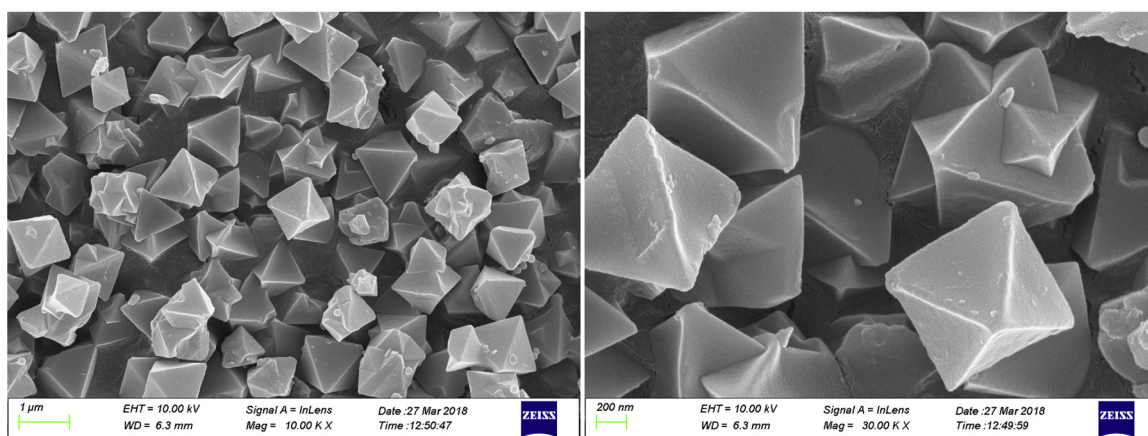
Then, the prepared catalysts were applied for the catalytic conversion of LA to EL. When the [Cu-BTC][HPM] catalyst (40 mg) was used for the esterification of LA (0.5 mmol) in ethanol (10 ml), a high EL yield of 92.4% could be obtained at $120\text{ }^\circ\text{C}$ in 4 h reaction time. On the other hand, when the reactions were carried out in the absence of additive or in the presence of Cu-BTC as catalyst, no EL product could be detected under the same reaction conditions ($120\text{ }^\circ\text{C}$, 4 h) (Table 2). Besides, a control experiment using pure HPM as catalyst was carried out, and the used amount of HPM was based on the content of HPM in the used [Cu-BTC][HPM]. It was found that the yield of EL was similar to that of using [Cu-BTC][HPM] as catalyst (Table 2). However, compared with HPM, [Cu-BTC][HPM] as catalyst can be effectively recycled in this reaction system. Thus, the as-prepared [Cu-BTC][HPM] catalyst exhibited good catalytic activity for the esterification of levulinic acid to ethyl levulinate.

Reaction temperature and reaction time are normally important factors influencing the reaction process. The effect of reaction temperature and reaction time on the catalytic conversion of LA to EL by the prepared [Cu-BTC][HPM] catalyst was examined, and the results are illustrated in Fig. 6. Increasing the reaction temperature or prolonging the reaction time allowed the esterification reaction to proceed more thoroughly.

In specific experiments, when the reaction was conducted at $80\text{ }^\circ\text{C}$, the conversion of LA to EL was so slow that only a maximum EL yield of 53.1% was obtained in 14 h reaction time. When the reaction temperature was increased to $100\text{ }^\circ\text{C}$, it took only four hours to reach the EL yield of 60.2%, and LA could almost be completely converted to EL in 12 h. When the reaction temperature was further increased to $120\text{ }^\circ\text{C}$, the yield of EL was close to 100% in 6 h reaction time, affording nearly 100% EL selectivity. According to the above experimental results, it can

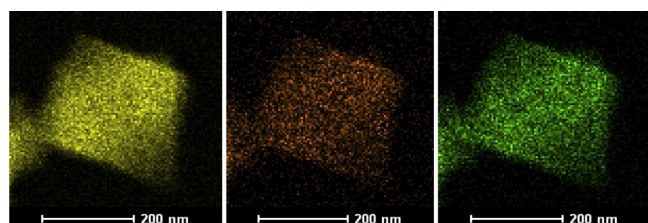


(a)



(b)

Fig. 3. SEM images of (a) Cu-BTC and (b) [Cu-BTC][HPM].



(a)

(b)

(c)

Fig. 4. EDX mapping of the [Cu-BTC][HPM], elemental mapping of (a) Cu, (b) P and (c) Mo.

be summarized that increasing the reaction temperature is more conducive to the improvement of the EL yield than prolonging the reaction time. Under the applied reaction conditions, EL is the only product, and common by-products such as angelica lactones, γ -valerolactone [39] and ethanol inter-molecular etherification products were not detected, which is consistent with the results reported in the references [27,40,41]. The esterification process of levulinic acid is an equilibrium reaction, but the addition of a sufficient amount of ethanol allows the reaction to proceed to the direction of EL formation, and the proper acidity of the catalyst also avoids the occurrence of other side reactions.

3.3. Effect of catalyst dosage on the catalytic conversion of LA to EL by [Cu-BTC][HPM] catalyst

The effect of the used amount of catalyst on the catalytic conversion of LA into EL was also investigated, and the results are shown in Fig. 7. The results suggested the reaction rate and product yield were positively correlated with the amount of catalyst used. When 20 mg [Cu-BTC][HPM] catalyst was used in the reaction, an EL yield of 79.5% could be achieved at 120 °C in 4 h reaction time. When the dosage of the catalyst was increased to 40 mg, the EL yield increased to 92.4% under the same reaction conditions. With the further increase of the catalyst amount to 80 mg, the LA was almost completely converted to EL (100% yield) at 120 °C for 4 h.

The reaction mechanism for the selective conversion of LA to EL in ethanol can be elaborated from the following aspects. The active component of the used catalyst is HPM, a strong Bronsted acid with hydrogen ion as active center. At the beginning of the catalytic reaction, protons attack levulinic acid to form carbonium ions. The nucleophilic oxygen atom of ethanol then attacks the levulinic acid intermediate [42], resulting in the formation of oxonium ions. The new oxonium ions produced by the proton transfer in the oxonium ions are further dehydrated, and the product ethyl levulinate is produced after deprotonation [42]. During the reaction, the metal-centered Cu, which has an unsaturated coordination number, can provide a certain amount of Lewis acid sites to adsorb levulinic acid, meanwhile increases the

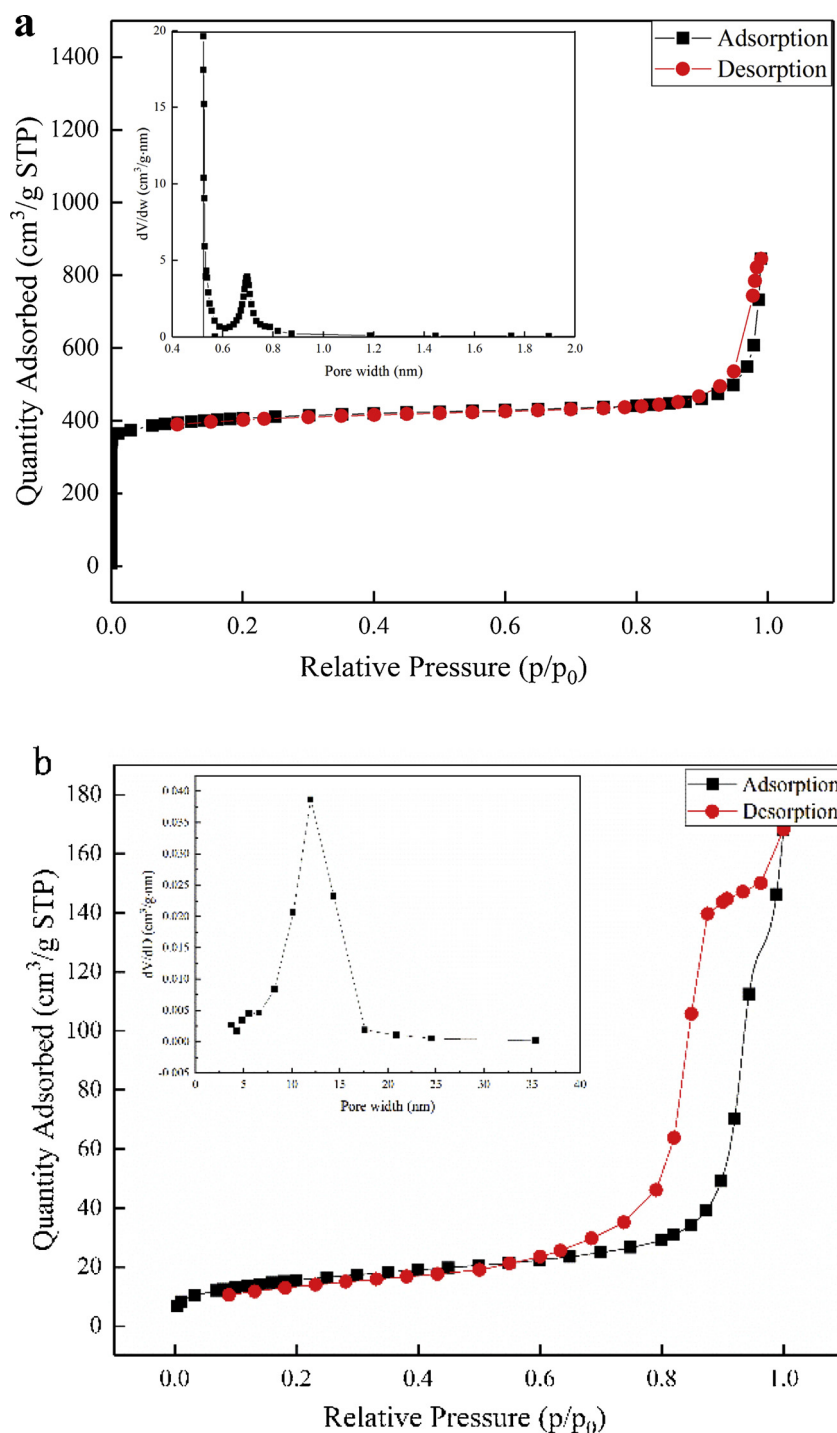


Fig. 5. N₂ adsorption-desorption isotherms and pore size distribution curves (inset) of (a) [Cu-BTC] and (b) [Cu-BTC][HPM].

Table 1

The textural properties of Cu-BTC and [Cu-BTC][HPM].

Sample	BET surface area (m ² /g)	Micropore area (m ² /g)	Total pore volume (cm ³ /g) [*]	Mesopore pore diameter (nm) ^{**}
Cu-BTC	1577	1493	1.13	25.8
[Cu-BTC][HPM]	57	26	0.23	11.4

* BJH adsorption cumulative volume of pores between 1.7 nm and 300 nm diameter.

** BJH adsorption average pore diameter (4V/A).

Table 2
Comparison of catalytic performance of various catalysts in this work.

Catalyst	Catalyst amount (mg)	LA conversion (%)	EL yield (mol %)
No catalyst	0	0	0
Cu-BTC	40	0	0
[Cu-BTC][HPM]	40	100	92.4
HPM	9	100	93.5

Reaction conditions: 0.5 mmol LA, 10 ml ethanol, 120 °C, 4 h.

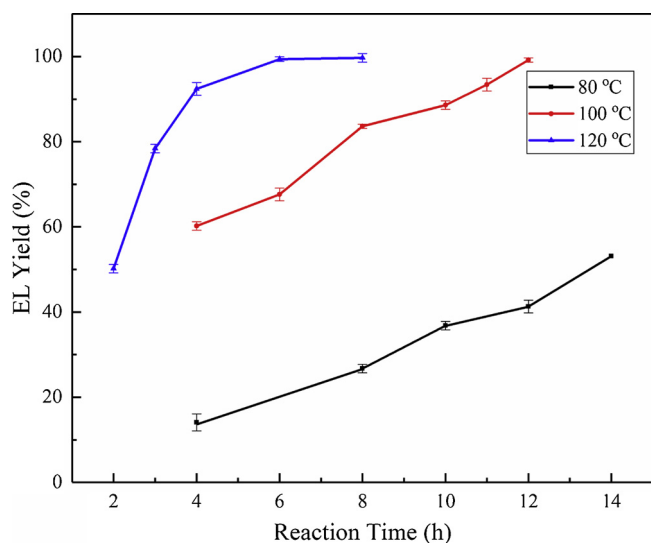


Fig. 6. Influence of reaction temperature and reaction time on the catalytic conversion of LA to EL by the [Cu-BTC][HPM] catalyst. Reaction conditions: 0.5 mmol LA, 40 mg catalyst, 10 ml ethanol.

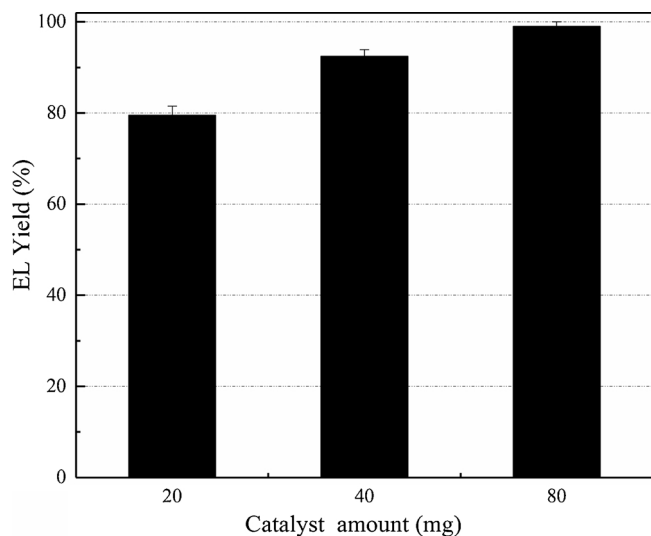


Fig. 7. Influence of the [Cu-BTC][HPM] amounts on the EL yield. Reaction conditions: 0.5 mmol LA, 10 ml ethanol, 120 °C, 4 h.

electrophilic properties of the carboxylic acid carbon atoms, to promote the esterification reaction.

3.4. Effect of initial substrate loading amount

The effect of initial LA loading amount (0.25–2 mmol) on the catalytic conversion of LA to EL by the [Cu-BTC][HPM] catalyst was investigated (Fig. 8). It can be seen that when a substrate loading amount as low as 0.25 mmol was applied, LA was selectively converted to EL,

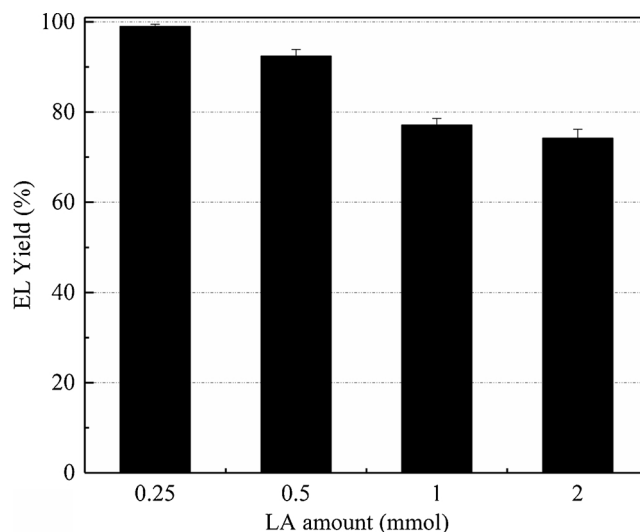


Fig. 8. Influence of the initial LA loading amounts on the EL yield. Reaction conditions: 40 mg [Cu-BTC][HPM], 10 ml ethanol, 120 °C, 4 h.

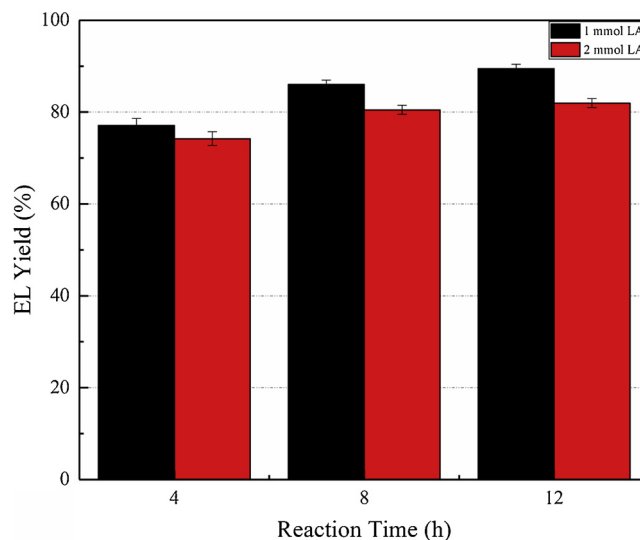


Fig. 9. Time-dependent changes in EL yields under different initial LA concentrations. Reaction conditions: 40 mg [Cu-BTC][HPM], 10 ml ethanol, 120 °C.

and almost 100% EL yield could be obtained at 120 °C in 4 h reaction time. When the LA amount was increased to 0.5 mmol, the EL yield could be remained at 92.4%, indicating that there were adequate catalytic active sites for the conversion of LA to EL. When the LA loading amount was increased to a higher level to 1 mmol and 2 mmol, the EL yields decreased to 77% and 74%, respectively, in 4 h reaction time, ascribing to the deficiency of the active component HPM for more substrate. After the reaction time was prolonged to 8 h and 12 h, the highest EL yield of 89% and 81% could be achieved with LA dosage of 1 mmol and 2 mmol, respectively (Fig. 9). Thus, the as-prepared [Cu-BTC][HPM] catalyst was applicable to the high initial LA loading for

Table 3
Performance of different catalysts in the esterification process of LA to EL.

Catalyst	Temp. (°C)	Time (h)	EL yield (mol %)	Ref.
20-HPW/Zr	150	3	97	[21]
UiO-66	60	2	> 99	[25]
H ₄ SiW ₁₂ O ₄₀ /SiO ₂	75	6	67	[43]
HPA/Silica	78	10	78	[42]
[Cu-BTC][HPM]	120	6	> 99	This work

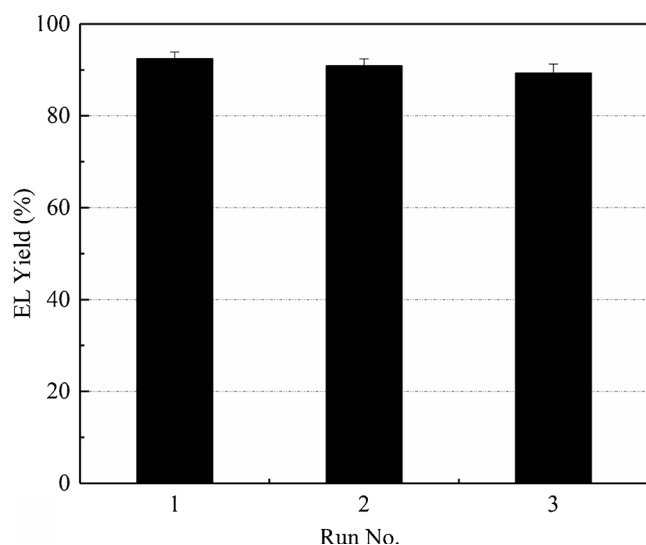


Fig. 10. Recycle performance of [Cu-BTC][HPM]. Reaction conditions: 0.5 mmol LA, 40 mg catalyst, 10 ml ethanol, 120 °C for 4 h.

Table 4
Element contents of [Cu-BTC][HPM] before and after the reaction by ICP*.

Elements	Contents (mg/g)	
	Before the reaction	After the reaction
Cu	151.9	158.6
Mo	151.6	150.8

* Uncertainty = 2%.

the production of EL in ethanol, and should be beneficial to the practical application.

The catalytic performance of [Cu-BTC][HPM] was also compared with the other heteropolyacid heterogeneous catalysts and MOF materials reported in the other published literatures as shown in Table 3, and it shows that the catalyst [Cu-BTC][HPM] exhibited excellent performance for the production of EL from LA in ethanol.

3.5. Catalyst recycling performance for conversion of LA to EL

The recycling performance of the catalyst was tested at 120 °C for 4 h. The spent catalyst was separated by centrifugation, and washed with ethanol, and then dried before reuse. The fresh catalyst could afford an EL yield of 92.4%. In the subsequent two cycles of use, EL yield decreased slightly but still maintained a relatively high yield of 89.5% when the reaction proceeded to the third time, as shown in Fig. 10. The catalyst after reuse was characterized by XRD, FTIR and ICP, and there was no distinct difference could be observed in their XRD patterns and FTIR spectra (Figures S2 and S3), confirming that the catalyst still maintains its crystal structure and properties after use. The element contents of the catalyst were analyzed by ICP to further examine whether the catalyst had changed after the reaction. The results are shown in Table 4. It reveals that after three times of the reaction, the change of Cu and Mo contents were almost negligible, which indicated that the Cu in the MOF did not precipitate and the MOF structure remained stable. Meanwhile the content of Mo, representing HPM, did not decrease, proving that HPM had no loss within the Cu-BTC structure. These analysis results demonstrate that the [Cu-BTC][HPM] catalyst was stable in the reaction system and gave fairly constant EL product yields. The slight decrease in EL yield in the recycled runs should probably be ascribed to the occupation of active site on the catalyst by LA or EL that was unable to be completely removed during the washing process, and thus resulted in the slight decrease of the

available active sites and EL yields.

4. Conclusions

In this work, a MOF-supported phosphomolybdic acid catalyst [Cu-BTC][HPM] was successfully synthesized using a one-step method at ambient temperature, with a metal-organic framework (Cu-BTC) as the carrier and a polyoxometalate HPM as the active component. The as-prepared [Cu-BTC][HPM] was used as catalyst for the esterification of biomass-derived LA to EL in ethanol, and achieved excellent results in that the yield of EL was close to 100% at 120 °C in 6 h reaction time. Owing to the highly ordered and suitable pore structure of Cu-BTC and the intense interaction between HPM and Cu-BTC, HPM is stably present in the MOF structure and has exhibited good performance in recycling test compared to homogeneous catalysts.

Acknowledgements

The authors appreciate the financial support from the National Natural Science Foundation of China (NSFC, No. 21876091, 51508284, 21577073), the Natural Science Fund for Distinguished Young Scholars of Tianjin (No. 17JCQJC45500), the Natural Science Foundation of Tianjin (No. 16JCZDJC33700), and Central Public Research Institutes Basic Funds for Research and Development (Agro-Environmental Protection Institute, Ministry of Agriculture, 22060302008023).

Appendix A. Supplementary data

Supplementary material related to this article can be found, in the online version, at doi:<https://doi.org/10.1016/j.apcata.2019.01.004>.

References

- [1] D.M. Alonso, J.Q. Bond, J.A. Dumesic, *Green Chem.* 12 (2010).
- [2] P. Gallezot, *Chem. Soc. Rev.* 41 (2012) 1538–1558.
- [3] C. Xu, R.A. Arancón, J. Labidi, R. Luque, *Chem. Soc. Rev.* 43 (2014) 7485–7500.
- [4] J.J. Bozell, G.R. Petersen, *Green Chem.* 12 (2010).
- [5] B. Liu, Z. Zhang, *ACS Catal.* 6 (2015) 326–338.
- [6] S. Alipour, H. Omidvarborna, *RSC Adv.* 6 (2016) 111616–111621.
- [7] F.H. Isikgor, C.R. Becer, *Polym. Chem-Uk* 6 (2015) 4497–4559.
- [8] F.D. Pileidis, M.M. Titirici, *ChemSuschem* 9 (2016) 562–582.
- [9] L. Yan, Q. Yao, Y. Fu, *Green Chem.* 19 (2017) 5527–5547.
- [10] J. Zhang, S. Wu, B. Li, H. Zhang, *Chemcatchem* 4 (2012) 1230–1237.
- [11] A. Démolis, N. Essayem, F. Rataboul, *ACS Sustain. Chem. Eng.* 2 (2014) 1338–1352.
- [12] C. Liu, Q. Feng, J. Yang, X. Qi, *Bioresour. Technol.* 255 (2018) 50–57.
- [13] F.R. Ma, M.A. Hanna, *Bioresour. Technol.* 70 (1999) 1–15.
- [14] Y. Kuwahara, W. Kaburagi, K. Nemoto, T. Fujitani, *Appl. Catal. A Gen.* 476 (2014) 186–196.
- [15] C.R. Patil, P.S. Niphadkar, V.V. Bokade, P.N. Joshi, *Catal. Commun.* 43 (2014) 188–191.
- [16] K. Manikandan, K.K. Cheralathan, *Appl. Catal. A Gen.* 547 (2017) 237–247.
- [17] M.N. Timofeeva, *Appl. Catal. A Gen.* 256 (2003) 19–35.
- [18] W. Deng, Q. Zhang, Y. Wang, *Dalton Trans.* 41 (2012) 9817–9831.
- [19] X. Zhang, Y. Li, L. Xue, S. Wang, X. Wang, Z. Jiang, *ACS Sustain. Chem. Eng.* 6 (2017) 165–176.
- [20] K.Y. Nandiwale, S.K. Sonar, P.S. Niphadkar, P.N. Joshi, S.S. Deshpande, V.S. Patil, V.V. Bokade, *Appl. Catal. A Gen.* 460–461 (2013) 90–98.
- [21] N.A.S. Ramli, D. Sivasubramaniam, N.A.S. Amin, *Bioenerg Res.* 10 (2017) 1105–1116.
- [22] H. Furukawa, K.E. Cordova, M. O’Keefe, O.M. Yaghi, *Science* 341 (2013) 1230444.
- [23] A.J. Howarth, Y. Liu, P. Li, Z. Li, T.C. Wang, J.T. Hupp, O.K. Farha, *Nat. Rev. Mater.* 1 (2016).
- [24] H.C. Zhou, J.R. Long, O.M. Yaghi, *Chem. Rev.* 112 (2012) 673–674.
- [25] F.G. Cirujano, A. Corma, F.X. Llabrés i Xamena, *Catal. Today* 257 (2015) 213–220.
- [26] S.S.Y. Chui, S.M.F. Lo, J.P.H. Charmant, A.G. Orpen, I.D. Williams, *Science* 283 (1999) 1148–1150.
- [27] D.R. Fernandes, A.S. Rocha, E.F. Mai, C.J.A. Mota, V. Teixeira da Silva, *Appl. Catal. A Gen.* 425 (2012) 199–204.
- [28] Z. Wang, Q. Chen, *Green Chem.* 18 (2016) 5884–5889.
- [29] H.B. Wu, B.Y. Xia, L. Yu, X.Y. Yu, X.W. Lou, *Nat. Commun.* 6 (2015) 6512.
- [30] J. Hu, H. Cai, H. Ren, Y. Wei, Z. Xu, H. Liu, Y. Hu, *Ind. Eng. Chem. Res.* 49 (2010) 12605–12612.
- [31] W. Huang, X. Zhou, Q. Xia, J. Peng, H. Wang, Z. Li, *Ind. Eng. Chem. Res.* 53 (2014) 11176–11184.
- [32] S. Lin, Z. Song, G. Che, A. Ren, P. Li, C. Liu, J. Zhang, *Microporous Mesoporous*

- Mater. 193 (2014) 27–34.
- [33] C.H. Specht, F.H. Frimmel, Phys. Chem. Chem. Phys. 3 (2001) 5444–5449.
- [34] L.T.L. Nguyen, T.T. Nguyen, K.D. Nguyen, N.T.S. Phan, Appl. Catal. A Gen. 425 (2012) 44–52.
- [35] G.R. Rao, T. Rajkumar, B. Varghese, Solid. State. Sci. 11 (2009) 36–42.
- [36] H. Du, J. Bai, C. Zuo, Z. Xin, J. Hu, CrystEngComm. 13 (2011) 3314–3316.
- [37] T. Tsuruoka, S. Furukawa, Y. Takashima, K. Yoshida, S. Isoda, S. Kitagawa, Angew. Chem. Int. Ed. Engl. 48 (2009) 4739–4743.
- [38] C.-Y. Sun, S.-X. Liu, D.-D. Liang, K.-Z. Shao, Y.-H. Ren, Z.-M. Su, J. Am. Chem. Soc. 131 (2009) 1883–1888.
- [39] E.S. Sankar, V. Mohan, M. Suresh, G. Saidulu, B.D. Raju, K.S.R. Rao, Catal. Commun. 75 (2016) 1–5.
- [40] J.A. Melero, G. Morales, J. Iglesias, M. Paniagua, B. Hernandez, S. Penedo, Appl. Catal. A Gen. 466 (2013) 116–122.
- [41] K.Y. Nandiwale, S.K. Sonar, P.S. Niphadkar, P.N. Joshi, S.S. Deshpande, V.S. Patil, V.V. Bokade, Appl. Catal. A Gen. 460 (2013) 90–98.
- [42] G. Pasquale, P. Vázquez, G. Romanelli, G. Baronetti, Catal. Commun. 18 (2012) 115–120.
- [43] K. Yan, G. Wu, J. Wen, A. Chen, Catal. Commun. 34 (2013) 58–63.